A vibro-impact electromechanical system: models of the random dynamics of an embarked pendulum

R. Lima, R. Sampaio, Christian Soize

HAL Id: hal-00903243
https://hal.science/hal-00903243

Submitted on 10 Nov 2013

A VIBRO-IMPACT ELECTROMECHANICAL SYSTEM: MODELS OF THE RANDOM DYNAMICS OF AN EMBARKED PENDULUM

Roberta Lima[1, 2]
Rubens Sampaio[1]
Christian Soize[2]
roberta.dequeirozlima@univ-paris-est.fr; rsampaio@puc-rio.br; christian.soize@univ-paris-est.fr;

1 - PUC-Rio, Department of Mechanical Engineering, Rua Marquês de São Vicente, 225, Gávea - 22453-900, Rio de Janeiro, RJ - Brazil

2 - Universit Paris-Est, Laboratoire Modlisation et Simulation Multi Echelle, MSME UMR 8208 CNRS, 5 bd Descartes, 77454 Marne-la-Valle, France

Abstract. This paper analyzes the impact behavior of an embarked pendulum in a vibro-impact electromechanical system considering the existence of epistemic uncertainties in the system parameters. The electromechanical system is composed by a cart whose motion is excited by a DC motor and a embarked pendulum into this cart. The suspension point of the pendulum is fixed in cart, so that exists a relative motion between them. The influence of the DC motor in the dynamic behavior of the system is considered. The coupling between the motor and the cart is made by a mechanism called scotch yoke, so that the motor rotational motion is transformed in horizontal cart motion over a rail. The pendulum is modeled as a mathematical pendulum (bar without mass and particle of mass m_p at the end). Two different systems are analyzed. In the first one, the pendulum moves freely inside the cart. In the second, a flexible barrier, attached to the cart, constrains the pendulum motion and may cause impacts. Due to the relative motion between the cart and the pendulum, it is possible that occurs impact between these two elements. A continuous contact dynamic model is developed and the impact is described using the spring-dashpot model. The nonlinearities of the problem, the difference between these two configurations and the impact energy are analyzed. In the stochastic analysis, the uncertain parameter is modeled as random variable and the Maximum Entropy Principle is used to construct its probability model. Monte Carlo simulations are employed to compute the mean and the 90% confidence interval of the displacements of the pendulum and of the angular speed of the motor shaft.

Keywords: nonlinear dynamics, coupled systems, vibro-impact, embarked mass, stochastic analysis

1. INTRODUCTION

The electromechanical coupling is common in our actual technology. The presence of nonlinearities arising from the mutual interaction of the coupled systems turns the research on this topic important to engineering practice and leads to very interesting dynamical systems (Rocard, 1943; Kononenko, 1969; Nayfeh and Mook, 1979; Fidlin, 2006; Hagedorn, 1988; Evan-Iwanowski, 1976; Cartmell, 1990).

This paper is organized as follows. Section 2 describes the two coupled electromechanical systems analyzed. Section 3 presents the results of the deterministic simulations developed to each one of them. The probabilistic model of the parameter that is considered uncertain is constructed in Section 4 and the results of the simulations of the stochastic systems are presented in Section 5. Section 6 presents some conclusions.

2. DYNAMIC OF THE COUPLED SYSTEM

Next, it is presented the elements of the two coupled systems (motor, cart, pendulum, and barrier). The coupling between the motor and the mechanical systems are shown and the two coupled problems are described and mathematically formulated as initial-value problems. One interesting feature is that the nonlinearity of the equations increases with d, the coupling parameter, a feature that is not evident from the equations. The impact behavior of the systems, shown in Fig. 9, will highlight this increase of nonlinearity.

2.1 Electrical system: motor DC

The mathematical modeling of DC motors is based on the Kirchhoff's law (Karnopp *et al.*, 2006). It is constituted by the equations

$$l\dot{c}(t) + r\,c(t) + k_e\dot{\alpha}(t) = v\,, \tag{1}$$

$$j_m \ddot{\alpha}(t) + b_m \dot{\alpha}(t) - k_t\, c(t) = -\tau(t) \,, \tag{2}$$

where t is the time, v is the source voltage, c is the electric current, $\dot{\alpha}$ is the angular speed of the motor, l is the electric inductance, j_m is the motor moment of inertia, b_m is the damping ratio in the transmission of the torque generated by the motor to drive the coupled mechanical system, k_t is the torque constant, k_e is the motor electromagnetic force constant and r is the electrical resistance. Figure 1 shows a sketch of a DC motor. The available torque to the coupled mechanical system is represented by τ, that is the component of the torque vector $\vec{\tau}$ in the z direction shown in Fig. 1.
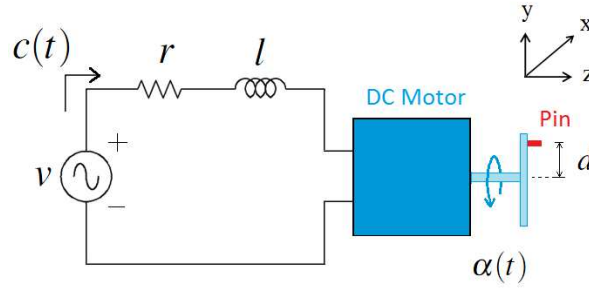

Figure 1. Electrical motor DC.

Assuming that the load applied in the motor and source voltage are constant in time, the motor achieves a steady state. Thus, the electric current and the angular speed become constant and $\ddot{\alpha}(t) = 0 = \dot{c}(t) = 0, \forall t \in \mathbb{R}^{\geq 0}$. By equations (1) and (2), the angular speed of the motor shaft and the current in steady state, respectively $\dot{\alpha}_{steady}$ and c_{steady}, can be calculated by

$$\dot{\alpha}_{steady} = \frac{-\tau\, r + k_t\, v}{b_m\, r + k_e\, k_t} \qquad , \qquad c_{steady} = \frac{v}{r} - \frac{k_e}{r}\left(\frac{-\tau\, r + k_t\, v}{b_m\, r + k_e\, k_t}\right). \tag{3}$$

When the hypothesis of constant load is not verified, the angular speed of the motor shaft and the current do not reach a constant value. This kind of situation happens when, for example, a mechanical system is coupled to the motor. In this case, $\dot{\alpha}$ and c variate in time in a way that the dynamics of the motor will be influenced by the coupled mechanical system.

Two more situations are relevant when we analyze electrical motors. The first one is when there is no load applied in the motor (i.e. $\tau(t) = 0, \forall t \in \mathbb{R}^{\geq 0}$) and the source voltage is constant in time. Then, the motor achieves its maximum angular speed that is called the *no load speed*. It is calculated by

$$\dot{\alpha}_{no\ load} = \frac{k_t\, v}{b_m\, r + k_e\, k_t} \,. \tag{4}$$

The second one is when the motor delivers the maximum torque. This torque is achieved when the load applied in the motor is such that the motor does not move at all. This is called the *stall torque*. If the source voltage is constant in time, it is calculated by

$$\tau_{stall} = \frac{k_t\, v}{r} \,. \tag{5}$$

In the problems discussed here, there is the constraint $\tau(t) < \tau_{stall}$. In Sec. 3 it is taken care do not reach this condition.

2.2 Coupled motor-cart-pendulum system

As described in the introduction, the system analyzed in this paper is composed by a cart whose motion is driven by a DC motor, sketched in Fig. 1, and a embarked pendulum into this cart. The motor is coupled to the cart through a pin that slides into a slot machined on a plexiglas plate that is part to the cart, as shown in Fig. 2. The pin hole is drilled off-center on a disk fixed in the axis of the motor, so that the motor rotational motion is transformed into horizontal cart motion over a rail.

The suspension point of the pendulum is fixed in the cart, so that exists a relative motion between them.

The embarked pendulum is modeled as a mathematical pendulum (bar without mass and particle of mass m_p at the end). The pendulum length is represented by l_p and the pendulum angular displacement by θ.
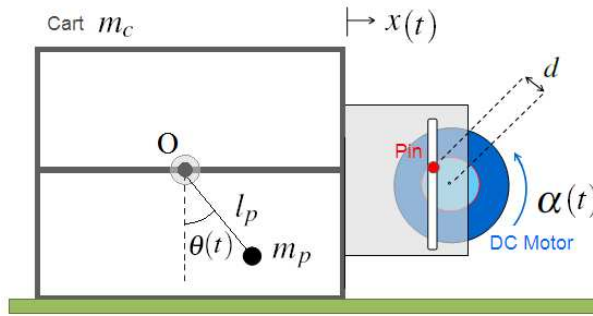
Figure 2. Coupled motor-cart-pendulum system.

The mass of the mechanical system, m, is equal the cart mass plus pendulum mass, $m_c + m_p$. The horizontal cart displacement is represented by x. Due to constraints, the cart is not allowed to move in the vertical direction.

Using the Lagrangian equation $\mathcal{L} = \mathcal{T} - \mathcal{V}$, with the angle θ and displacement x of the cart as generalized coordinates, the kinetic and potential energies of the mechanical cart-pendulum system are defined respectively as

$$\mathcal{T} = \frac{1}{2}m_p[(l_p\dot{\theta}\cos\theta + \dot{x})^2 + (l_p\dot{\theta}\sin\theta)^2] + \frac{1}{2}m_c\dot{x}^2 \ , \tag{6}$$

$$\mathcal{V} = -m_p g(l_p\cos\theta) \ , \tag{7}$$

where g is the acceleration of gravity. Thus, the equation of the cart-pendulum are

$$m_p l_p^2 \ddot{\theta}(t) + m_p l_p \ddot{x}(t)\cos\theta(t) + m_p g l_p \sin\theta(t) = 0 \ , \tag{8}$$

$$(m_p + m_c)\ddot{x}(t) + m_p l_p \ddot{\theta}(t)\cos\theta(t) - m_p l_p \dot{\theta}^2(t)\sin\theta(t) = f(t) \ , \tag{9}$$

where, f represents the horizontal coupling force between the DC motor and the cart. It is possible observe that the relative motion of the embarked pendulum causes a variation in the position of the center of mass of the mechanical system.

To model the coupling between the motor and the mechanical system, it is assumed that the motor shaft is rigid. Thus, the available torque to the coupled mechanical system, $\vec{\tau}$, can be written as

$$\vec{\tau}(t) = \vec{d}(t) \times \vec{f}(t) \ , \tag{10}$$

where $\vec{d}$ is the eccentricity of the pin of the motor and $\vec{f}$ is the coupling force between the DC motor and the cart. By the problem geometry, the module of $\vec{d}$ is the nominal eccentricity of the pin, i.e. $||\vec{d}|| = d$. Besides this, the component of $\vec{d}$ that is perpendicular to the plane of the cart movement is always zero and, the others horizontal and vertical components can be calculated from the angular displacement α of the motor.

Assuming that there is no friction between the pin and the slot machined on an acrylic plate, the vector $\vec{f}$ only has a horizontal component, f (the horizontal force that the DC motor exerts in the cart). Thus, $\vec{d}$ and $\vec{f}$ are written as

$$\vec{d}(t) = \begin{bmatrix} d\cos\alpha(t) \\ d\sin\alpha(t) \\ 0 \end{bmatrix} \qquad \vec{f}(t) = \begin{bmatrix} f(t) \\ 0 \\ 0 \end{bmatrix} \ . \tag{11}$$

Substituting Eq. (11) in Eq. (10), the module of $\vec{\tau}(t)$ is

$$\tau(t) = -f(t)d\sin\alpha(t) \ . \tag{12}$$

Due to the problem geometry, the horizontal motion of the cart, x, and the angular displacement of the motor, α, are related by the constraint

$$x(t) = d\cos\alpha(t) \, . \tag{13}$$

Substituting the Eq. (12), (13), (8) and (9) in the equations of the electric motor, we obtain a system of differential equations for the coupled system.

Given the source voltage of the motor, v, the dynamic of the coupled system is written in terms of the variables α, c and θ. Thus, the initial value problem for the motor-cart-pendulum-barrier system is: given the source voltage of the motor, v, find (α, c, θ) satisfying

$$l\dot{c}(t) + rc(t) + k_e\dot{\alpha}(t) = v \, ,$$

$$\ddot{\alpha}(t)\left[j_m + (m_c + m_p)d^2(\sin\alpha(t))^2\right] + \dot{\alpha}(t)\left[b_m + (m_c + m_p)d^2\dot{\alpha}(t)\cos\alpha(t)\,\sin\alpha(t)\right]$$
$$-k_t\, c(t) - \ddot{\theta}(t)\left[m_p l_p\cos\theta(t)d\sin\alpha(t)\right] + \dot{\theta}(t)\left[m_p\, l_p\dot{\theta}(t)\sin\theta(t)d\sin\alpha(t)\right] = 0 \, , \tag{14}$$

$$\ddot{\theta}(t)\left[m_p\, l_p^2\right] - \ddot{\alpha}(t)\left[m_p\, l_p\,\cos\theta(t)d\sin\alpha(t)\right] - \dot{\alpha}(t)\left[m_p\, l_p\cos\theta(t)d\cos\alpha(t)\dot{\alpha}(t)\right]$$
$$+ m_p\, g\, l_p\sin\theta(t) \,=\, 0 \, ,$$

for given initial conditions.

2.3 Coupled motor-cart-pendulum-barrier system

In the coupled system described in the previous subsection, the pendulum can move freely inside the cart. In this section, a flexible barrier is attached to the cart, constraining the pendulum motion. In this application, the barrier is inside the cart. Due to the relative motion between the cart and the pendulum, it is possible that occur impacts between the pendulum and the barrier, as suggested in Fig. 3.
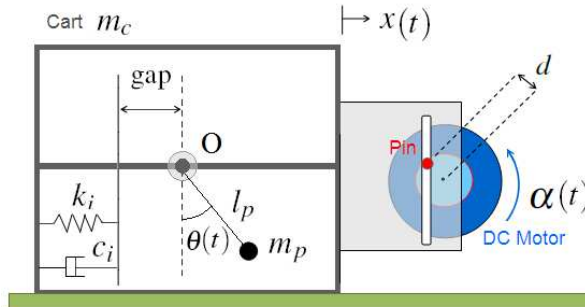

Figure 3. Coupled motor-cart-pendulum-barrier system.

A continuous contact dynamic model is developed and the impact is described using the spring-dashpot model. The spring-damper element of the impact is represented by a spring with stiffness k_i and a damper with damping coefficient c_i. Some hypotheses are adopted in this shock model. It is assumed that

- the impact is central and co-linear;

- the impact velocity is along the impact line (so there is no impact velocity component in the tangential axis).

The equation of the cart-pendulum-barrier system are

$$m_p l_p^2\ddot{\theta}(t) + m_p l_p\ddot{x}(t)\cos\theta(t) + m_p g l_p\sin\theta(t) = f_{\text{imp}}(t)l_p\cos\theta(t) \, , \tag{15}$$

$$(m_p + m_c)\ddot{x}(t) + m_p l_p\ddot{\theta}(t)\cos\theta(t) - m_p l_p\dot{\theta}^2(t)\sin\theta(t) = f(t) \, , \tag{16}$$

where, f represents the horizontal coupling force between the DC motor and the cart and f_{imp} the impact force exerted in the pendulum. This force is written as:

$$f_{\text{imp}}(t) = -\phi\left[\, k_i\,(l_p\sin\theta(t) + \text{gap}) + c_i\,(l_p\dot{\theta}(t)\cos\theta(t))\right] \, , \tag{17}$$

$$\phi = \begin{cases} 1, & if \quad -l_p \sin\theta(t) > \text{gap}, \\ 0, & if \quad -l_p \sin\theta(t) \leq \text{gap}, \end{cases} \tag{18}$$

in it gap is the horizontal distance from the suspension point to the equilibrium position of the barrier.

As in the previous coupled system, the cart is not allowed to move in the vertical direction. Due to the problem geometry, the horizontal motion of the cart and the angular displacement α of the motor are related by Eq. (13).

Once again, it is assumed that the motor shaft is rigid and that there is no friction between the pin and the slot machined on the acrylic plate. Thus, the available torque to the coupled mechanical system, $\vec{\tau}$, is written as Eq. (12).

Substituting the Eq. (12), (13), (15) and (16) in the equations of the electric motor, we obtain a system of differential equations for the coupled system.

Given the source voltage of the motor, v, the dynamic of the coupled system is written in terms of the variables α, c and θ. Thus, the initial value problem for the motor-cart-pendulum system is: given the source voltage of the motor, v, find (α, c, θ) satisfying

$$l\dot{c}(t) + rc(t) + k_e\dot{\alpha}(t) = v,$$

$$\ddot{\alpha}(t)\left[j_m + (m_c+m_p)d^2(\sin\alpha(t))^2\right] + \dot{\alpha}(t)\left[b_m + (m_c+m_p)d^2\dot{\alpha}(t)\cos\alpha(t)\sin\alpha(t)\right]$$
$$-k_t\,c(t) - \ddot{\theta}(t)\left[m_pl_p\cos\theta(t)d\sin\alpha(t)\right] + \dot{\theta}(t)\left[m_p\,l_p\dot{\theta}(t)\sin\theta(t)d\sin\alpha(t)\right] = 0, \tag{19}$$

$$\ddot{\theta}(t)\left[m_p\,l_p^2\right] - \ddot{\alpha}(t)\left[m_p\,l_p\,\cos\theta(t)d\sin\alpha(t)\right] - \dot{\alpha}(t)\left[m_p\,l_p\cos\theta(t)d\cos\alpha(t)\dot{\alpha}(t)\right]$$
$$+ m_p\,g\,l_p\sin\theta(t) + \phi k_i(l_p\sin\theta(t)+\text{gap})l_p\cos\theta(t) + \phi c_i(l_p\dot{\theta}(t)\cos\theta(t))l_p\cos\theta(t) = 0.$$

3. NUMERICAL SIMULATIONS OF THE DYNAMICS OF THE COUPLED SYSTEMS

To better comprehend the behavior of the coupled systems composed by the DC motor and the mechanical systems, we begin analyzing the deterministic models. Simulations of the two systems are compared in order to observe the influence of the pendulum in the rotational motion of the motor shaft.

The specifications of the motor parameters used in all simulations were obtained from the specifications of the motor Maxon DC brushless number 411678. The source voltage was assumed to be constant in time and equal to 2.4 [Volt].

Eq. 14 and 19 were numerically integrated by a fourth-order Runge-Kutta method. The initial conditions assumed for the current in the motor, for the angular position and velocity of the motor shaft and pendulum were, in all simulations

$$\alpha(0) = 0.0\,[\text{rad}], \qquad \dot{\alpha}(0) = 0.0\,[\text{Hz}], \qquad c(0) = v/r = 7.81\,[\text{Amp}], \qquad \theta(0) = \frac{\pi}{2}\,[\text{rad}], \qquad \dot{\theta}(0) = 0.0. \tag{20}$$

According to the numerical findings in (Lima and Sampaio, 2012), when d is sufficiently small, as 0.001 [m], the behavior of the motor-cart-pendulum system approaches to the linear case. The current and velocity of the motor shaft oscillates over time with a very small amplitude. But when d is bigger, the amplitude of the oscillations of $\dot{\alpha}$ and c grows and the non-linear behavior of system is highlighted.

In the following analysis of the motor-cart-pendulum system, the nominal eccentricity of the pin was consider to be 0.01 [m] and the pendulum length was assumed to be 0.075 [m]. The values of the cart and the pendulum masses were $m_c = 0.0$ [Kg] and $m_p = 5.0$ [Kg], so that the total mass, $m = m_c + m_p = 5.0$ [Kg], is equal to the embarked mass.

3.1 Simulations of the motor-cart-pendulum system

The system of Eq. 14 was numerically integrated in a range of $[0.0, 10.0]$ seconds. Figures 4(a) and 4(b) show the obtained results to the pendulum displacement and to the velocity of the motor shaft over time.

3.2 Simulations of the motor-cart-pendulum-barrier system

As done to the motor-cart-pendulum system, the system of Eq. 19 was numerically integrated in a range of $[0.0, 15.0]$ seconds with $d = 10^{-3}$. The values of the stiffness and damping coefficient used in the simulations were $k_i = 10^6$ [N/m] and $c_i = 0$ [Ns/m], so that there is no energy dissipation in the impact model.

Two different values of the parameter gap/l_p were investigated: 0.0 and 0.5. The obtained results to the pendulum displacement and to the velocity of the motor shaft are shown in Fig.5(a), 5(b), 6(a), 6(b), 7(a), 7(b), 8(a) and 8(b).
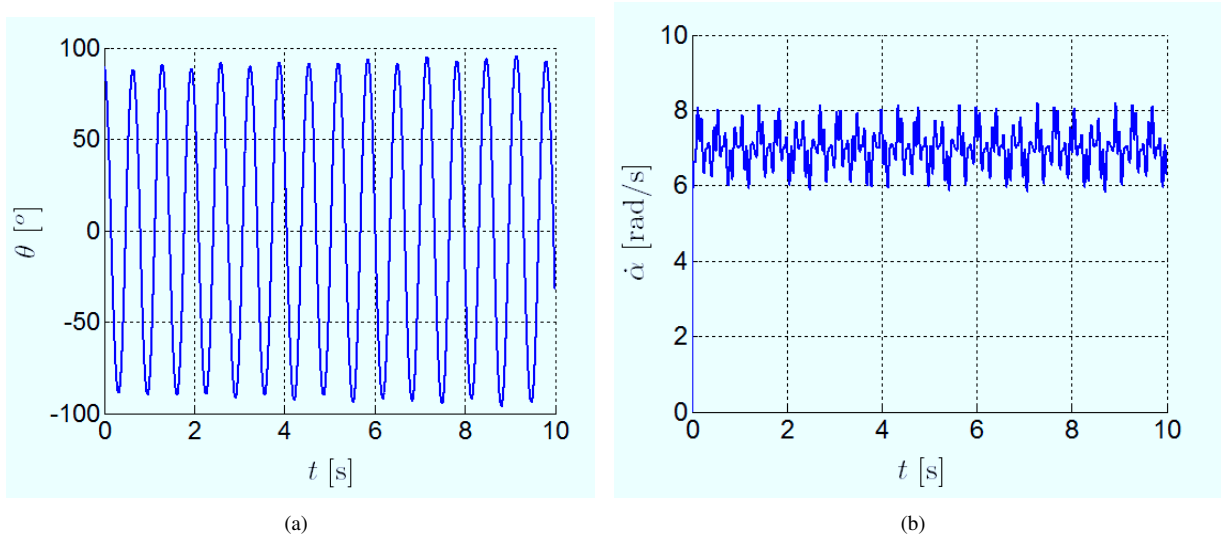
Figure 4. Coupled motor-cart-pendulum system with $d = 10^{-3}$ [m]: (a) pendulum displacement and (b) velocity of the motor shaft over time.
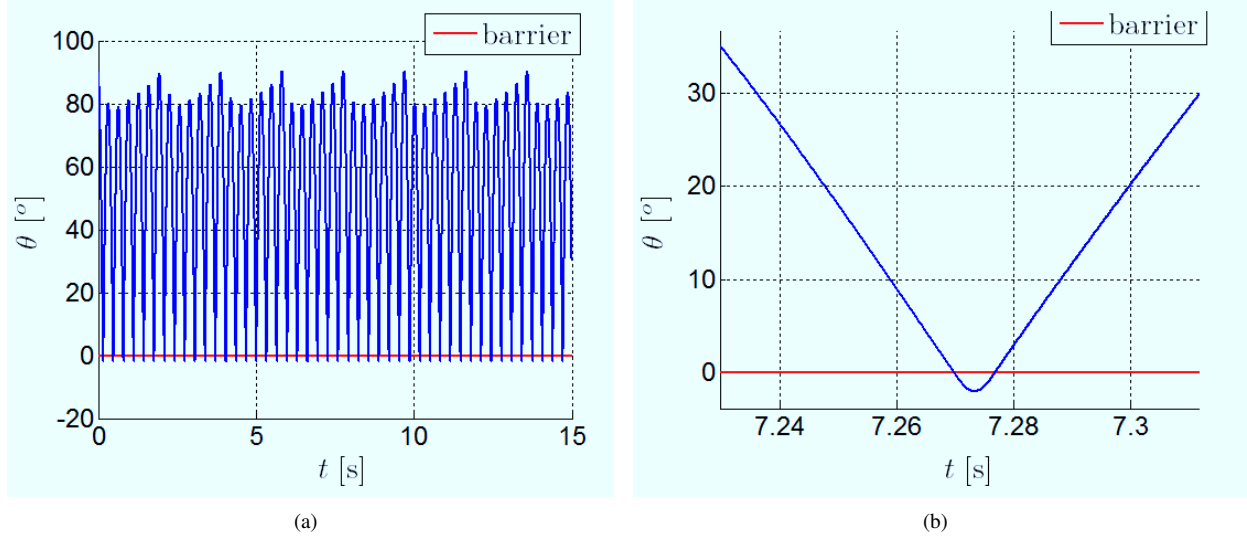

Figure 5. Coupled motor-cart-pendulum-barrier system with $\text{gap}/l_p = 0$: (a) pendulum displacement over time and initial position of the barrier (b) zoom of an impact.

Comparing the obtained results in the two configurations, it is possible to observe that changes in value of the parameter gap/l_p can modify a lot the response of the system, as the maximum amplitude of the pendulum displacement, maximum velocity of the motor shaft and therefore, the impact behavior of the system.

To quantify the influence of gap/l_p in the impact behavior, systems with different values of gap were compared in terms of the average of the maximum impact energy reached in each impact.

In a simulation, the maximum impact energy during the j-th impact, $\varepsilon_{\text{imp}}^j$, occurs when the spring k_i is compressed to the maximum, that is, when $l_p \sin(\theta)$ achieves its minimum value during the j-th impact. Noting as $\theta^\star$ the angle of the pendulum corresponding to this configuration of maximum compression, $\varepsilon_{\text{imp}}^j$ is calculated by

$$\varepsilon_{\text{imp}}^j = \frac{1}{2} k_i \left(l_p \sin(\theta^\star) + gap \right)^2, \qquad \text{if} \quad -l_p \sin\theta^\star > \text{gap} . \tag{21}$$

The average of the maximum impact energy during the whole simulation is calculated by

$$\mathcal{E} = \frac{\sum_{j=1}^{N_{\text{imp}}} \varepsilon_{\text{imp}}^j}{N_{\text{imp}}} , \tag{22}$$

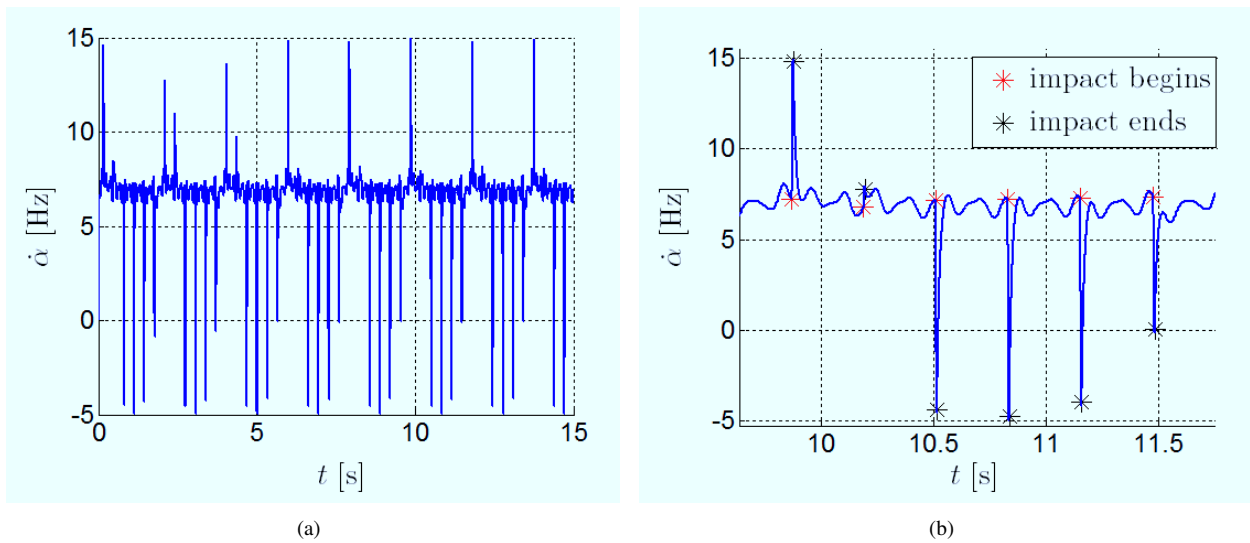where N_{imp} is the total number of impacts during the simulation.

(a)

(b)

Figure 6. Coupled motor-cart-pendulum-barrier system with $\text{gap}/l_p = 0$: (a) velocity of the motor shaft over time and (b) zoom of some impacts.
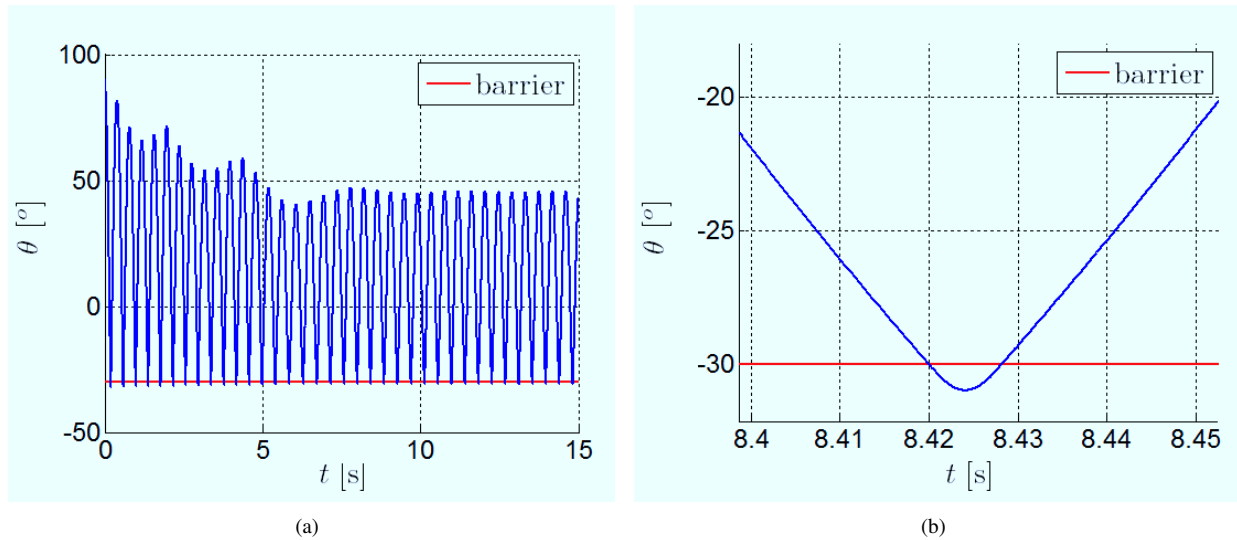

(a)

(b)

Figure 7. Coupled motor-cart-pendulum-barrier system with $\text{gap}/l_p = 0.5$: (a) pendulum displacement over time and initial position of the barrier and (b) zoom of an impact.

Figure 9 shows the normalized graph of the average of the impact energy in function of the parameter gap/l_p for different values of the nominal eccentricity of the pin, d. Worth noting that $d = 0$ [m] means no coupling between the motor and the cart. Also, as seen in Lima and Sampaio (2012), the bigger is d, bigger are the nonlinearities involved in the system.

Observing Fig. 9, it is possible to note that for values of d near zero, as 10^{-5} [m] and 10^{-4} [m], the graph of the impact energy is very similar to the graph with $d = 0$ [m]. The average impact energy presents its maximum at $\text{gap}/l_p = 0$ and its minimum when $\text{gap}/l_p = 1$. These results were expected, since when $\text{gap}/l_p = 1$ there is no impact and since when $\text{gap}/l_p = 0$, the pendulum begins the impact in the vertical position, exactly when it has its maximum velocity. When d is bigger, as 2×10^{-4} [m], 5×10^{-4} [m], 8×10^{-4} [m] and 10^{-3} [m], the form of the graph of the average of the impact energy changes completely. The maximum do not occur anymore at $\text{gap}/l_p = 0$.

4. PROBABILISTIC MODEL

To make a stochastic analysis of the two proposed systems, a system parameter is considered uncertain. It is assumed that the stiffness in the spring-damper element of the impact, k_i, is a random variable represented by the capital letter K_i.

The Maximum Entropy Principle (PEM) is used to construct the probability density function of this random variable (Jaynes, 1957; Shannon, 1948). It is assumed that the available information are
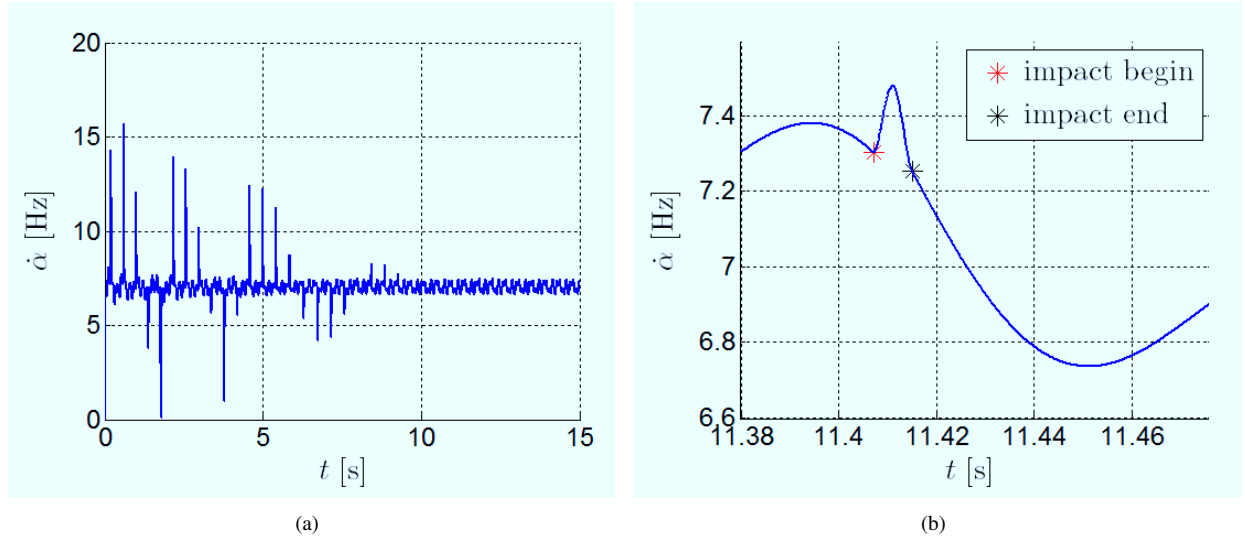
1. the stiffness value is always positive: $K_i > 0$;

Figure 8. Coupled motor-cart-pendulum-barrier system with $gap/l_p = 0.5$: (a) velocity of the motor shaft over time and (b) zoom of an impact.

2. the mean value is known: $E[K_i] = \mu$;

3. the response of the system is a second order random variable, that is the inverse problem is well posed: $E[K_1^{-2}] < \infty$.

Therefore, the Maximum Entropy Principle using Shannon entropy measure of the probability density function, p, of K_i yields the Gamma probability density function, given by

$$p(k_i) = \mathbb{1}_{[0,+\infty)}(k_i) \frac{1}{\mu} \left(\frac{1}{\delta^2} \right)^{\frac{1}{\delta^2}} \frac{1}{\Gamma(1/\delta^2)} \left(\frac{x}{\mu} \right)^{\frac{1}{\delta^2}-1} \exp \left(\frac{x}{\delta^2 \mu} \right) ,\tag{23}$$

where $\mathbb{1}_{[0,+\infty)}(k_i)$ is an indicator function that is equal to 1 for $k_i \in [0,+\infty)$ and 0 otherwise, and

- Γ is the Gamma function: $\Gamma(a) = \int_0^\infty t^{a-1} \exp(-t) \mathrm{d}t$;

- $\delta = \frac{\sigma}{\mu}$ is the coefficient variation (σ is the standard deviation).

5. NUMERICAL SIMULATIONS OF THE STOCHASTIC MOTOR-CART-PENDULUM-BARRIER SYSTEM

As it was assumed that the stiffness of the spring, k_i, in the barrier model is a random variable, the output variables of the stochastic coupled system are random processes with parameter t. Therefore, the pendulum displacement is represented by the random process Θ, the angular displacement of the motor shaft by A and the angular velocity of the motor shaft by $\dot{A}$. The average of the impact energy is also a random variable, and it is represented by $\mathcal{E}$.

To make the stochastic analysis, Monte Carlo simulations were employed to compute statistics of the response of the stochastic coupled system. In the simulations, the mean value K_i was assumed to be 10^6 [N/m] and its coefficient variation, $\delta = 0.25$.

Figures 10, 11(a) and 11(b) show the normalized histogram $\mathcal{E}$ and the envelope graphs of $Theta$ and $\dot{A}$ constructed with 150 realizations of these random process. In each realization, the system Eq. (19), was integrated in a range of $[0.0, 5.0]$ seconds with gap $= 0$. It is possible observe that the variations on stiffness of the spring bring dispersions to the oscillation amplitudes of $Theta$ and $\dot{A}$. Also, it is remarkable that there is a dispersion in the instants of begin and end of the impacts. The computed mean and variance of E were respectively 3.255 and 0.047 (units in J).

6. CONCLUSIONS

The purpose of this paper was to analyze the behavior an embarked pendulum in a vibro-impact electromechanical system in two different situations.

Two different systems were analyzed. In the first one, a pendulum moves freely inside the cart. In the second, a flexible barrier, attached to the cart, constrains the pendulum motion and causes impacts.

In the deterministic analysis, the influence of the parameter gap/l_p in the impact behavior were investigated for different values of the nominal eccentricity of the pin, d, the parameter that governs the nonlinearity of the system. As d
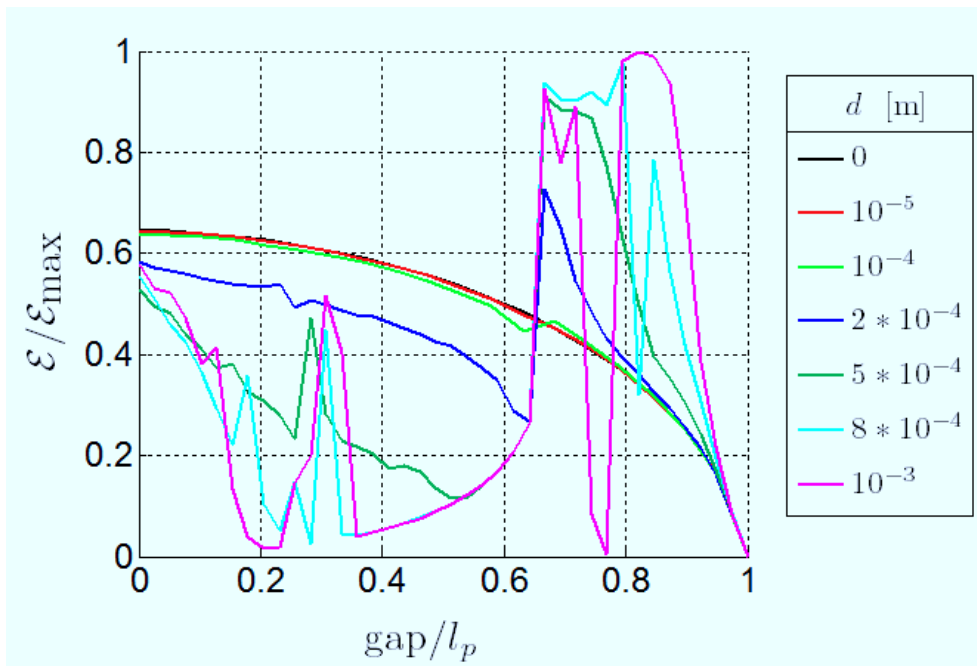
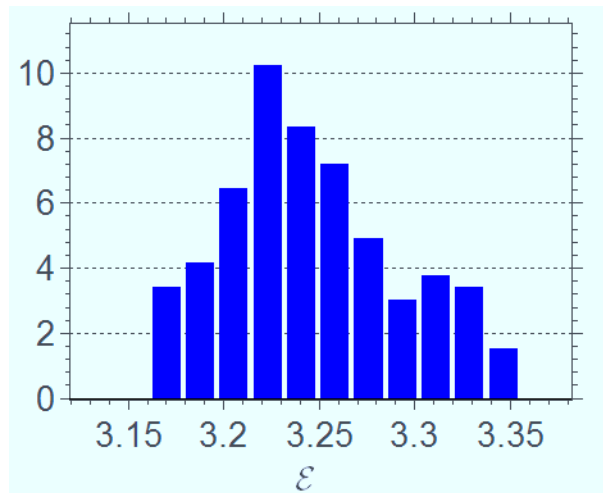Figure 9. Normalized average of the impact energy in function of the parameter gap/l_p.

Figure 10. Normalized histogram of $\mathcal{E}$.

increases the nonlinearity also increases. It was verified that for values of d near zero, the graph of the impact energy is very similar to the graph with $d = 0$ [m], that can be nicely predicted from conservation of energy. However, as d increases the form of the graph changes completely and in an unexpected fashion. This peculiar behavior is due to the energy taken by the pendulum from the motor. The energy of the mechanical systems varies a lot and the pumping of energy, from the motor to the mechanical system, increases with d. The systems analysed show a self-oscillation behavior, in the sense that the generation and maintenance of the motion comes from the motor but the oscillations have control of the energy taken from the motor. It varies with d that is a measure of the nonlinearity of the system. It is worth mentioning that the energy intake is at frequency zero, the constant voltage, but this energy is distributed for all frequencies due to the impacts. Due to lack of space, the energy analysis of this problem will be done in a follow-up paper.

In the stochastic analysis, the stiffness of the spring k_i, in the barrier was modeled as a random variable and the propagation of uncertainties in the coupled motor-cart-pendulum-barrier system was computed through Monte Carlo simulations. It is observed that the variations on stiffness of the spring brought dispersions in the instants of begin and end of the impacts and to the oscillation amplitudes of the pendulum displacement and velocity of the motor shaft.
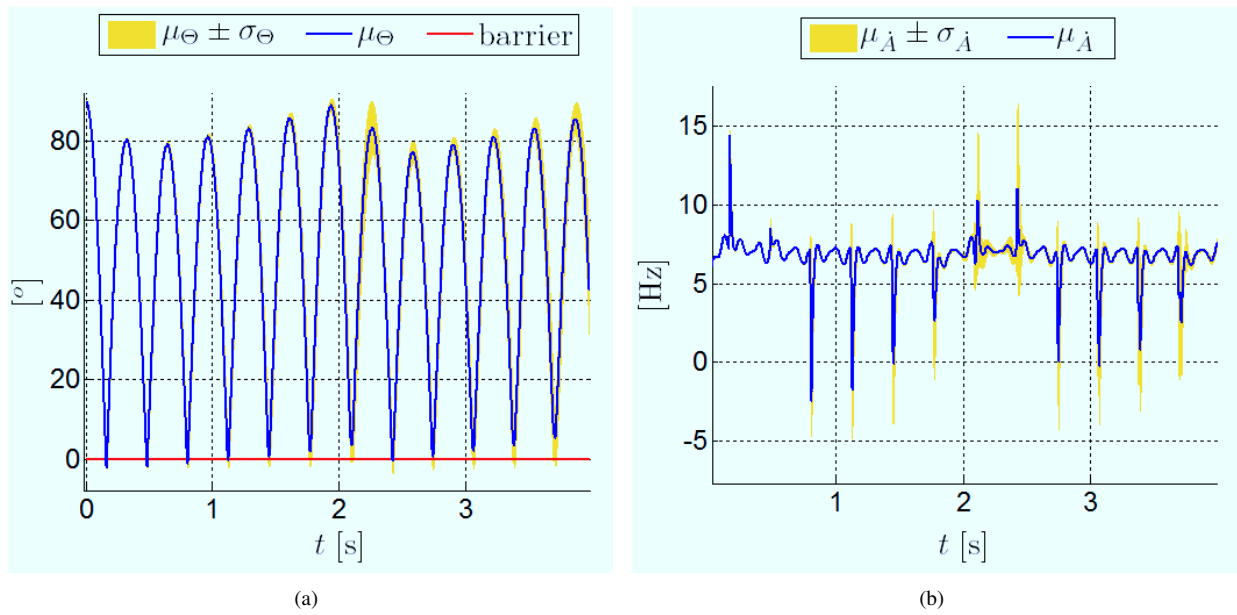
Figure 11. Motor-cart-pendulum-barrier system: (a) Envelope graphs of Θ and (b) $\dot{A}$.

7. ACKNOWLEDGEMENTS

8. REFERENCES

Cartmell, M., 1990. *Introduction to Linear, Parametric and Nonlinear Vibrations*, Vol. 260. Springer.

Evan-Iwanowski, R.M., 1976. *Resonance oscillations in mechanical systems*. Elsevier Publ. Co., Amsterdam.

Fidlin, A., 2006. *Nonlinear Oscillations in Mechanical Engineering*. Springer, Netherlands.

Hagedorn, P., 1988. *Non-linear Oscillations*. Clarendon Press, Oxford, 2nd edition.

Jaynes, E., 1957. "Information theory and statistical mechanics". *The Physical Review*, Vol. 106, No. 4, pp. 620–630.

Karnopp, D., Margolis, D. and Rosenberg, R., 2006. *System Dynamics: Modeling and Simulation of Mechatronic Systems*. John Wiley and Sons, 4th edition, New-York, USA.

Kononenko, V.O., 1969. *Vibrating Systems with a Limited Power Supply*. London Iliffe Books LTD, England.

Lima, R. and Sampaio, R., 2012. "Analysis of an Electromechanic Coupled System with Embarked Mass". *Mecânica Computacional,*, Vol. XXXI, pp. 2709–2733.

Nayfeh, A.H. and Mook, D.T., 1979. *Nonlinear Oscillations*. John Wiley and Sons, USA.

Rocard, Y., 1943. *Dynamique Générale des Vibrations*. Masson et Cie., Éditeurs, Paris, France.

Shannon, C., 1948. "A mathematical theory of communication". *Bell System Tech.*, Vol. 27, pp. 379–423 and 623–659.

9. RESPONSIBILITY NOTICE